buildings

Article

Utilization of Fly Ash from Lignite Combustion in Materials Sealing Hydro-Technical Structures

Zbigniew Kledyński, Agnieszka Machowska and Paweł Falaciński *

Faculty of Building Services, Hydro and Environmental Engineering, Warsaw University of Technology, Nowowiejska St. 20, 00-653 Warsaw, Poland; zbigniew.kledynski@pw.edu.pl (Z.K.); agnieszka.machowska@pw.edu.pl (A.M.)
* Correspondence: pawel.falacinski@pw.edu.pl

Abstract: In Poland, approximately 2 million hectares of agricultural land are at risk of flooding, which constitutes approximately 7% of the country's area, half of which is protected by flood embankments. The total length of the embankments is approximately 8.5 thousand km. kilometers. The age of the embankments and their related technical condition, as well as insufficient funds allocated for maintenance and renovation, mean that the flood risk in the areas protected by the embankments is higher than would result from the geometric parameters of the embankments and floods assumed for their design. The need to renovate embankments, including their sealing, causes an increase in interest in new technological and material solutions, and it is expected that these solutions will be pro-ecological: low-emission and consistent with the idea of a circular economy. The research was aimed at presenting the possibility of using fly ash from lignite combustion (low-rank coal) in Pątnów Power Plant, in raw form and fractions separated from it. The article presents the method of preparation and properties of hardening slurries containing mineral by-products of coal combustion. The tests showed the usefulness of the fly ashes used as the main component of hardening slurries. Additionally, a beneficial effect of the fine fraction (0–30 µm) of fly ash on the properties of the slurry, especially on tightness and hydraulic conductivity, was found.

Keywords: hardening slurry; fly ash; circular economy

check for updates

Citation: Kledyński, Z.; Machowska, A.; Falaciński, P. Utilization of Fly Ash from Lignite Combustion in Materials Sealing Hydro-Technical Structures. *Buildings* **2023**, *13*, 2589. https://doi.org/10.3390/buildings13102589

Academic Editor: Xingwei Li

Received: 7 September 2023
Revised: 10 October 2023
Accepted: 11 October 2023
Published: 13 October 2023

1. Introduction

The modernization of flood embankments, which protect economically valuable areas from flooding, usually consists of the implementation of an anti-filtration barrier in the embankment body and/or in its base, which significantly reduces or stops the flow of water. The most commonly used method of embankment modernization is the method of deep soil-grout mixing (DSM), in which a drill bit is inserted into the ground to a predetermined depth and, during mixing, cement slurry is fed through it [1,2]. The cut-off walls formed by this method are in the form of a palisade about 80 cm thick and several meters high. Using this method allows you to control the amount of grout consumption, but it does not give the possibility of soil compaction.

Another method of making the barrier is the WIPS method, in which a steel section is sunk into the embankment body or at its base by means of vibrations [3]. When the profile is pulled out, the resulting space is filled with the hardening slurry. The use of this method allows for compaction of the substrate, elimination of voids and loosening within a range of up to several meters from the barrier. Due to the use of heavy equipment and vibrations during the construction of the barrier, this method cannot be used in the vicinity of existing facilities. Moreover, there is a risk of tightening the gap, sedimentation of the hardening slurries and keying of the cover, i.e., lack of continuity as a result of deviation of the successive recesses of the profile from the vertical.

The cut-off wall can also be made using the slot method in a narrow excavation in two variants: using the continuous slot method deepened with an excavator or the so-called trencher (multi-bucket excavator of continuous operation) and at the same time feeding the slurry into the excavation through a pipeline; the method of successive sections in which the excavation is made and filled with slurry in sections implementing every other section in the first phase, and closing sections in the second phase [3,4]. Due to the composition of the slurry, two technologies are used in the successive sections method: a single-phase technology consisting of digging a trench under the cover of a hardening slurry which is then left to set and harden into a proper barrier, or a two-phase technology (with two variants) consisting in digging a trench under a cover bentonite-water slurry (phase I) which in the next phase is displaced from the excavation by the hardening slurry (phase II), which is the proper material of the barrier, or consists in sinking the excavation under the cover of the bentonite-water slurry, and then producing a working slurry in the excavation hardening by adding cement grout.

The cut-off wall is also made using the high-pressure jet injection method [5,6]. In the first stage of implementation, the soil is loosened with a stream of water or cement grout fed under pressure through a special nozzle, and in the next stage, it is mixed with cement grout. Solids of any shape can be formed in the ground using this method. The impact range of the stream is approx. 3–4 m and depends on the type of soil and the variant of the technology used.

An important aspect of the modernization of flood embankments is the use of innovative construction and material solutions. As a construction material for both vertical and horizontal cut-off walls, hardening slurries are used, mixtures of water, bentonite and binder, which thanks to the ingredients used, perform various functions [3,7,8]:

- drilling mud that keeps the hole or narrow excavation in the ground stable, which is ensured by the addition of bentonite (until the binding process begins), which gives the suspension thixotropic properties,
- structural material of the cut-off wall, which during hardening of the binder reaches a certain strength and anti-filtration properties.

The liquid slurry should have an appropriate density to ensure the stability of the excavation walls, as well as resistance to water loss due to self-weight displacement. Equally important from the point of view of the slurry preparation and transport to the place of incorporation is its viscosity. In most cases, the specific composition of the hardening slurry is determined experimentally depending on the properties it is to have. This process is particularly important when fillers or mineral additives are used to make the slurry, which affects the technological and functional properties of the slurry [2,7,9].

Research indicates the desirability of refining ashes by their fractionation, which can improve their quality and extend the scope of use [10–12].

2. Materials and Methods

Tap water, CEM I 42.5R cement, sodium bentonite (DYWONIT S) and fly ash from conventional combustion of lignite in the Pątnów Power Plant were used to prepare the hardening slurries being the subject of the tests. Hardening slurry recipes are shown in Table 1.

Table 1. Recipes of hardening slurries.

Component	R1P1	R1P2	R1P0	R2P1	R2P2	R2P0	R3P1	R3P2	R3P0
Water [kg]	1000	1000	1000	1000	1000	1000	1000	1000	1000
Bentonite [kg]	40	40	40	40	40	40	40	40	40
CEM I 42.5 [kg]	160	160	160	170	170	170	180	180	180
Fly ash 0–30 μm [kg]	300	-	-	380	-	-	450	-	-
Fly ash 30–100 μm [kg]	-	300	-	-	380	-	-	450	-
Fly ash [kg]	-	-	300	-	-	380	-	-	450

The fly ash used is characterized by spherical grains, which result from coal combustion at a temperature of approx. 1100 °C in pulverized coal boilers. Unfractionated ash with a grain size of 0–100 µm (marked P0) and ash fractionated in two grain size ranges: 0–30 µm (marked P1) and 30–100 µm (marked P2) were used in the tests. Table 2 shows the oxide composition of the ash.

Table 2. Chemical composition of unfractionated ash (P0) and fractions 0–30 µm (P1) and 30–100 µm (P2).

Properties [%]	P0	P1	P2
SiO_2	54.31	70.10	64.98
Al_2O_3	6.64	5.57	6.04
Fe_2O_3	5.34	5.24	5.69
CaO	21.25	12.02	14.61
MgO	3.86	2.29	2.68
SO_3	5.77	2.57	3.13
K_2O	0.43	0.41	0.43
Na_2O	0.10	0.07	0.10
P_2O_5	0.18	0.12	0.17
TiO_2	0.97	0.70	0.79
Mn_3O_4	0.30	0.17	0.20
SrO	0.13	0.06	0.08
BaO	0.13	0.07	0.10
Loss on ignition	0.52	0.56	0.95

The pozzolanic activity of the ash fraction 30–100 µm (marked P2) did not meet the requirements of the EN 450-1 standard, in contrast to the ash of the fraction 0–30 µm (marked P1).

The designed suspensions were tested in the liquid phase in order to determine the technological properties, and after hardening to determine the functional properties.

Liquid slurry tests were performed using:

- A baroid arm scale according to [13,14], used to measure the bulk density of the slurry (Figure 1a);
- A marsh funnel according to [13,14], used to measure the conventional viscosity of the slurry; the test consists of measuring the outflow time (in seconds) of 1000 mL of binder from a volume of 1500 mL placed in a funnel (Figure 1b);
- A cylinder with a fixed capacity of 1000 mL in accordance with [9], used to measure the daily water settling by determining (in % of volume) the amount of water separated spontaneously from the slurry after 24 h from pouring it into the cylinder and leaving it motionless (Figure 1b);
- A filter press in accordance with [13,14], which allows to determine the amount of filter filtrate (slurry loss in % of volume) coming out as a result of pressure from the freshly prepared slurry.

The samples for testing the slurries after hardening were made in steel molds d = h = 80 mm and PVC. Until set, the samples were stored in molds under a foil cover in a laboratory room. After 2–3 days, the samples were removed from the steel molds and immersed completely in tap water at a temperature of 18 ± 2 °C, in which they matured until testing. The samples made in plastic (PVC) molds and intended for testing hydraulic conductivity were not removed from the molds, but placed with them in water and stored in this way until the test.

Samples of slurries after 28 and 90 days of maturation were tested:

- compressive strength in accordance with the PN-EN 12390-3 standard [15]; the samples, after being taken out of the tub with water, were surface dried, then weighed and measured; if it was necessary, the upper surface of the sample was leveled by applying a layer of gypsum grout so as to ensure a precise fit of the surface of the tested sample to the head of the testing machine (Figure 2a);
- splitting tensile strength in accordance with PN-EN 12390-6 standard [16] (Figure 2b);

- hydraulic conductivity [17–19]- test with a variable hydraulic gradient; hydraulic conductivity was determined from Equation (1):

$$k_T = \frac{a \cdot L}{A \cdot \Delta t} \ln \frac{h_1}{h_2} \quad (1)$$

where k_T—hydraulic conductivity at a temperature of T (m/s); a—supply tube sectional area (m^2); L—tested sample height (m); A—sample cross-sectional area (m^2) Δt = $t_2 - t_1$—time between hydraulic pressure measurements h_1, h_2 (s); h_1, h_2—hydraulic pressure values at t_2, t_1 (m); T—filtration liquid temperature (°C).

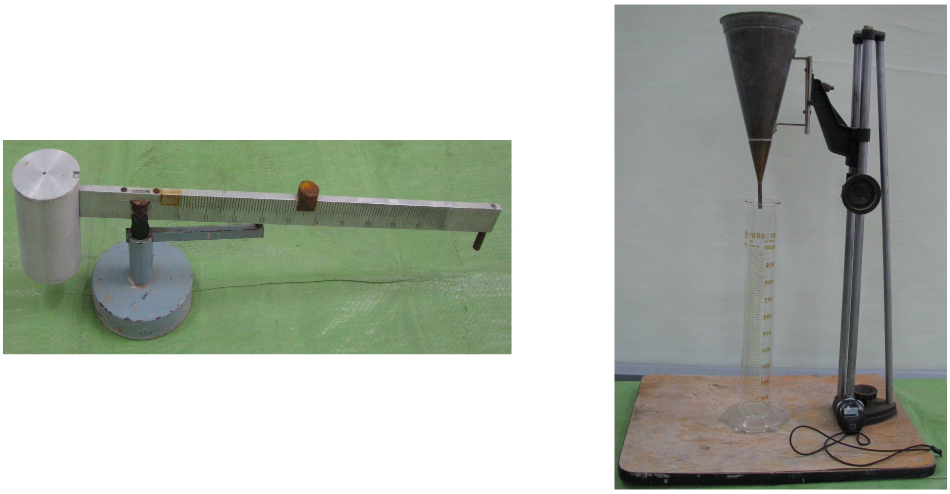

(**a**) (**b**)

Figure 1. Devices for testing the properties of liquid hardening slurries: (**a**) Baroid arm scale, (**b**) Marsh funnel with cylinder with a fixed capacity of 1000 mL.

(**a**) (**b**)

Figure 2. Samples of the hardening slurries during testing: (**a**) compressive strength, (**b**) splitting tensile strength.

The influence of the temperature of the filtering liquid was taken into account by converting the k_T values obtained at the water temperature T into the k_{10} values corresponding to the temperature of +10 °C, according to Equation (2):

$$k_{10} = \frac{k_T}{0.7 + 0.03T} \quad (2)$$

where k_{10}—hydraulic conductivity at a temperature of +10 °C (m/s).

The diagram for testing the hydraulic conductivity of the hardening slurries and the author's apparatus is shown in Figure 3.

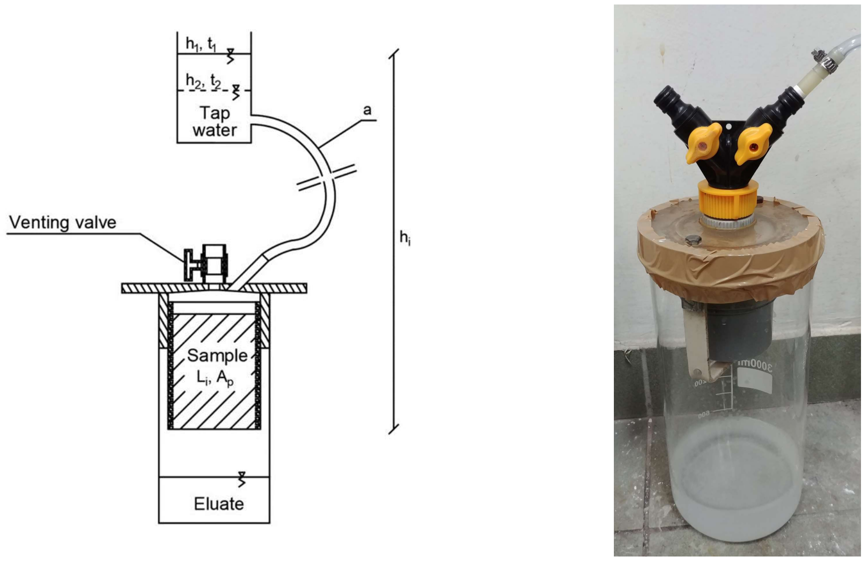

(**a**) (**b**)

Figure 3. The diagram for testing the hydraulic conductivity of the hardening slurries (**a**) and the author's apparatus (**b**).

- phase composition by X-ray diffraction (XRD) in a Philips PW 1130 apparatus with a CuKα cathode, wavelength 15.4 Å, in the angular range 5–60° 2θ with a step of 0.05° 2θ, tuning time 3 s/step; beam parameters: 16 mA and 35 kV; samples pre-crushed in a mortar were dried in a desiccator and then ground to the size of grains passing through a 0.063 mm sieve;
- microstructures using the FEI Nova NanoSEM 200 scanning electron microscope, in the low vacuum technique in a water vapor atmosphere with a pressure of 60 Pa; samples were not dried before testing, and fresh fractures were observed, on which a thin layer of carbon was sputtered to ensure electrical conductivity;
- mercury porosimetry using the Carlo Erba 2000 apparatus in the pressure range up to 2000 atm; samples were dried in a desiccator to constant weight.

3. Discussion

The results of testing the technological properties of hardening slurries are presented in Table 3.

Table 3. Technological properties of the tested hardening slurries.

Recipe	Sample Numbers	Density ρ [g/cm^3]	Conventional Viscosity L (s)	Water Loss 24 h O_d [%]	Slurry Loss in % of Volume P [%]
R1P1	1	1.29	47	2.0	58.4
R1P2	2	1.28	39	7.5	61.4
R1P0	3	1.29	40	11.0	61.9
R2P1	4	1.34	52	2.0	53.6
R2P2	5	1.33	41	13.0	56.8
R2P0	6	1.33	42	10.0	56.3
R3P1	7	1.37	60	2.0	49.9
R3P2	8	1.36	43	12.0	51.8
R3P0	9	1.36	45	6.0	52.9

The densities of slurries in the liquid state are sufficient to ensure the stability of the excavation—Table 3. The density of slurries increases with the increase in the amount of dosed ash and cement. In the case of formulas of the R1 group—samples 1–3—the density remains within the range of 1.28 ÷ 1.29 g/cm^3, with a solids content of 500 kg per 1000 kg of water, in the case of formulas R2—samples 4–6—the density is within in the range of 1.33 ÷ 1.34 g/cm^3, with the solids content of 590 kg/1000 kg of water, and in the group of formulas R3—samples 7–9—the density is in the range of 1.36 ÷ 1.37 g/cm^3, with solids content 670 kg/1000 kg water. At fixed contents of solid components, the highest density values are found in slurries made with fractionated ash 0–30 µm (P1)—samples (R1P1, R2P1 and R3P1).

With reference to the assumptions adopted in the design of slurry recipes [3,7,9], the conventional viscosity should be within the range enabling the use of hydraulic transport of the slurry to the place of incorporation—Table 3, Figure 4. The highest viscosity value is achieved by slurries made with fractionated ash 0–30 µm (P1), while the lowest viscosity is presented by slurries made with fractionated ash 30–100 µm (P2)—samples (R1P2, R2P2 and R3P2); the use of fine-grained ashes in relation to coarser or non-fractionated ashes results in an increase in viscosity in the range of 8–17 s. Viscosity values of suspensions with P2 ash and unfractionated ash (P0) are similar.

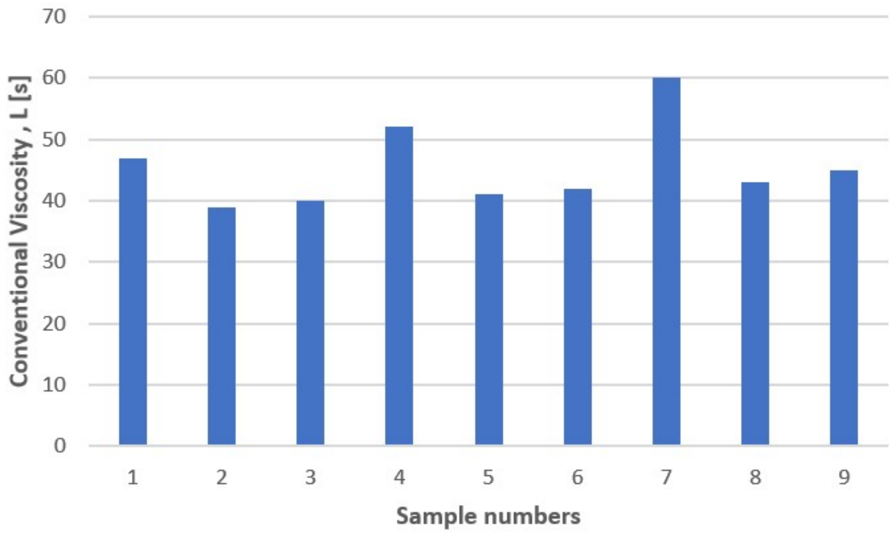

Figure 4. Conventional viscosity of the tested samples of the hardening slurries; sample numbers according to Table 3.

By analyzing the values of daily water settling (Table 3 and Figure 5) of individual slurries, it can be seen that the ash grain size has a significant impact on the value of this parameter. The lowest value of daily water settling is shown by slurries made with P1 ash, and their settling practically does not change despite different dosing of solid components (binder and ash). In the case of P2 ash, a significant increase in the value of daily standstill was noted, in the range of 7.5–13%, depending on the content of solids. High settling values, in the range of 6–11%, are achieved by slurry with unfractionated ash P0 (samples 3, 6, 9). However, while the daily standstill of slurries with ash P2 (samples 2, 5, 8) increases with the increase in the dosage of solid particles (binder and ash), the daily standstill of slurries with unfractionated ash P0 (samples 3, 6, 9) decreases with increasing solids content. This is the result of an increase in the share of the fine fraction of P1 ash in the recipe which contains the largest number of colloidal particles, eliminated from the recipes with P2 ash.

Analyzing the percentage losses of the liquid slurry, resulting from the pressure (in the range of 1–5 bar) displacement of the mixing water from the slurry (Table 3), it can be concluded that this loss decreases with the increase in the dosing of solid particles, including colloidal ones. The slurry made with the addition of ash of the 0–30 µm fraction (P1) is more resistant to water displacement under the influence of pressure in relation to the slurry with the ash of the 30–100 µm fraction (P2) and with non-fractionated ash (P0). This observation corresponds well with the behavior of slurries with spontaneous separation of water in the settling tests because in both tests the decisive influence on the result is the content of the finest solid particles capable of forming a colloidal gel.

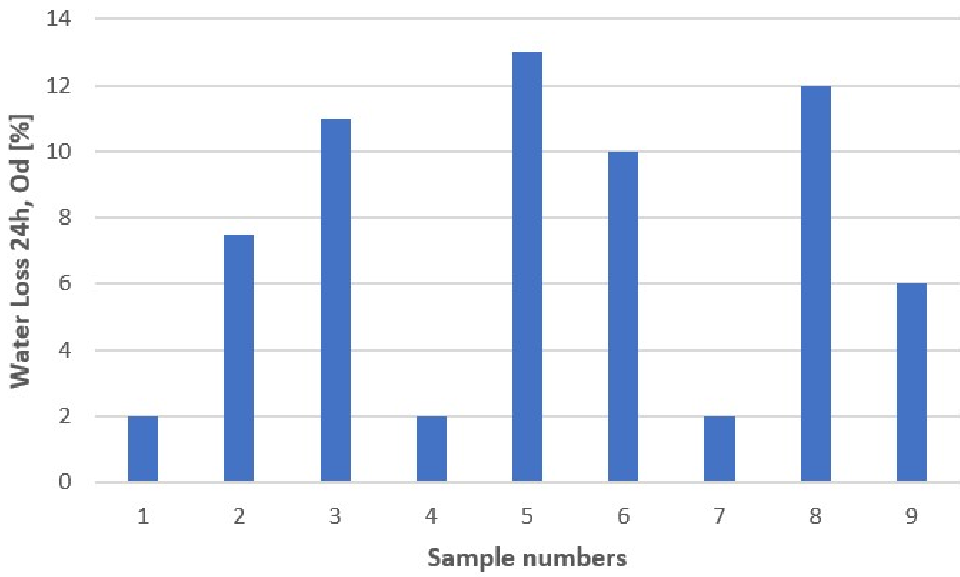

Figure 5. Water Loss (24 h) of the tested samples of the hardening slurries; sample numbers according to Table 3.

Analyzing the values obtained in the tests of the technological parameters of the liquid slurry (density, conventional viscosity, water loss 24 h, filtration resistance), it can be concluded that almost all recipes are suitable for use as material for cut-off walls made with the most commonly used methods, i.e., slot method), deep mixing method (DSM) or vibration method (narrow gap method) [3,4]. Only sample no. 7 (with P1 ash, fraction 0–30 µm) may cause some difficulties (due to high viscosity) in pipe transport of the slurry to the place of its incorporation. However, this is not an insurmountable limitation, and to some extent depends on technical possibilities (equipment, distance between the slurry production center and the place of incorporation).

The basic performance parameters of the tested hardening slurries (after hardening) are presented in Table 4. The coefficient of variation for the calculated values is given in parentheses.

Table 4. Useful properties of hardening slurries.

Properties		1 R1P1	2 R1P2	3 R1P0	4 R2P1	5 R2P2	6 R2P0	7 R3P1	8 R3P2	9 R3P0
f_c [MPa]	28 days	0.22 (±9%)	0.20 (±23%)	0.22 (±8%)	0.31 (±17%)	0.33 (±7%)	0.30 (±4%)	0.39 (±18%)	0.39 (±6%)	0.40 (±2%)
	90 days	0.41 (±3%)	0.48 (±7%)	0.36 (±9%)	0.60 (±5%)	0.66 (±10%)	0.54 (±9%)	0.79 (±7%)	0.93 (±3%)	0.74 (±3.5%)
f_{ct} [MPa]	28 days	0.04 (±12%)	0.06 (±8%)	0.05 (±10%)	0.05 (±18%)	0.07 (±13)	0.05 (±10%)	0.05 (±18%)	0.09 (±6%)	0.09 (±16%)
	90 days	0.05 (±24%)	0.08 (±10%)	0.11 (±8%)	0.10 (±21%)	0.15 (±11%)	0.12 (±10%)	0.14 (±11%)	0.19 (±6%)	0.13 (±25%)
k_{10} [MPa]	28 days	4.81×10^{-8} (±15%)	2.28×10^{-7} (±8%)	2.60×10^{-7} (±15%)	2.73×10^{-8} (±19%)	2.29×10^{-7} (±20%)	1.26×10^{-7} (±19%)	1.01×10^{-8} (±18%)	1.48×10^{-7} (±24%)	1.08×10^{-7} (±11%)
	90 days	8.92×10^{-9} (±22%)	9.93×10^{-8} (±7%)	7.77×10^{-8} (±23%)	4.93×10^{-9} (±18%)	3.22×10^{-8} (±25%)	6.15×10^{-8} (±18%)	3.65×10^{-9} (±20%)	4.59×10^{-8} (±17%)	2.83×10^{-8} (±16%)

The compressive strengths f_c—after 28 days of curing—are very similar to each other and amount to about 0.20 MPa (recipe R1), about 0.30 MPa (recipe R2) and about 0.40 MPa (recipe R3). A clear increase in strength can be observed in correlation with the increase in the dosage of the binder. Analyzing the effect of maturation time on the values of compressive strength, an increasing tendency can be observed for all tested slurries. The increase in compressive strength between 28 and 90 days of maturation was similar for all recipes and ranged from 42 to 61%.

Figure 6 shows changes in the values (trends—fit lines) of the compressive strength f_c of hardening slurries depending on the p/c ratio (ash/cement). An increase in the f_c value is visible with an increase in the p/c ratio, for all ash grain sizes and between the dates of strength testing (28 and 90 days of maturation).

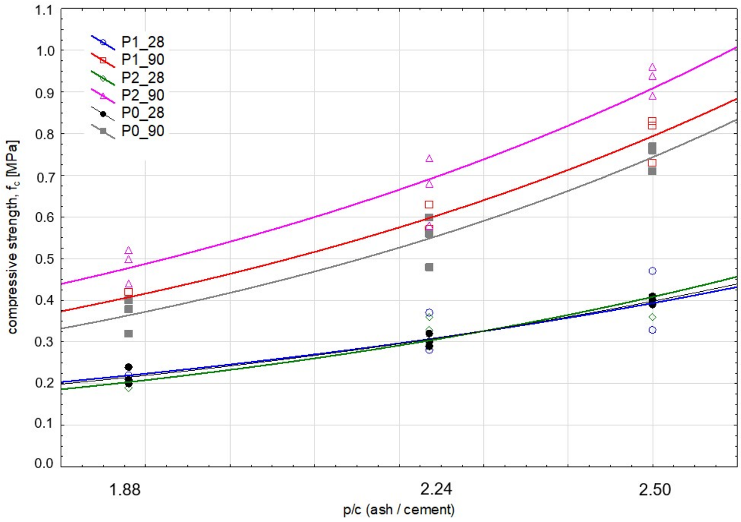

Figure 6. Changes in compressive strength f_c of hardening slurries depending on the p/c ratio and between the two ripening periods.

The values of the tensile strength (when splitting) f_{ct}—after 28 days of maturation—are generally similar (Table 4 and Figure 7). As with compressive strength, the f_{ct} values increase with increasing binder dosing. The influence of the maturing time on the tensile strength values is expressed in an upward trend.

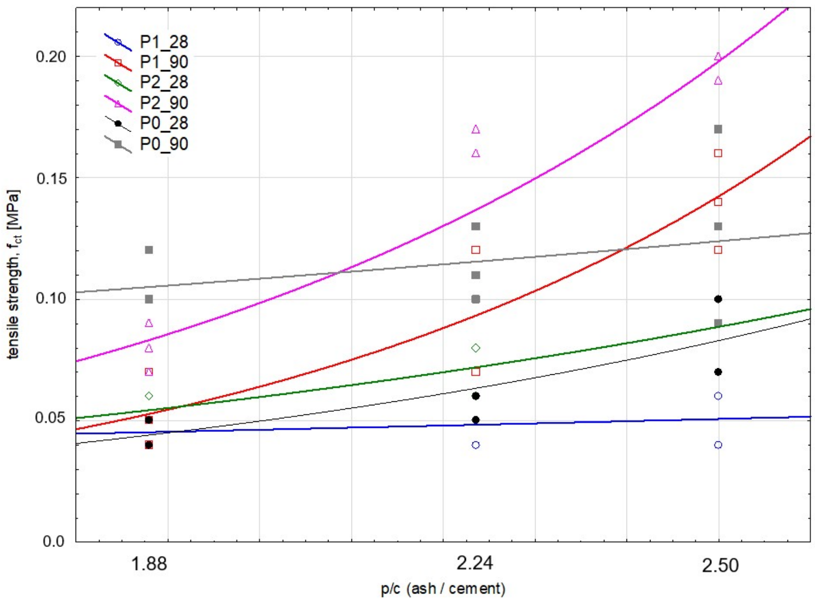

Figure 7. Changes in tensile strength f_{ct} of hardening slurries depending on the p/c ratio and between the two ripening periods.

Analyzing the values of hydraulic conductivity of the tested slurries (Table 4 and Figure 8), it can be seen that the k_{10} values after 28 days of maturation differed by an order of magnitude between samples containing ash of fine fraction 0–30 μm (P1)—samples 1, 4, 7 (order 10^{-8} m/s), and the remaining samples from groups R1, R2 and R3 with unfractionated ash or coarser fraction 30–100 μm (P2)—samples 2 and 3, 5 and 6 and 8 and 9, respectively (order 10^{-7} m/s). After 90 days of maturation, the difference in the order of magnitude remained between the groups described above, but all slurries sealed, i.e., samples with fine fraction ash (in all groups R1, R2 and R3) showed hydraulic conductivity k_{10} of 10^{-9} m/s, and the remaining 10^{-8} m/s. The positive effect of increasing the dosing of solid components on the tightness of slurries was also confirmed. The lowest value of hydraulic conductivity had the slurry R3P1: 3.65 $\times$ 10^{-9} m/s (sample 7).

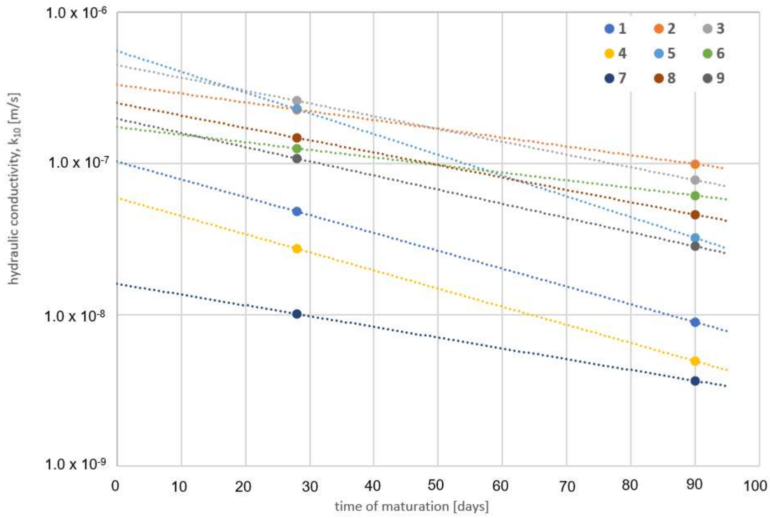

Figure 8. Changes in hydraulic conductivity k_{10} over time—trend lines, numbers: 1–9 recipe numbers.

The observed differences in the values of compressive and tensile strength and hydraulic conductivity of slurries made with different fractions of ash (determined after 90 days of maturation) were confirmed in the phase composition and microstructure studies of the slurries [4]. The results obtained by X-ray diffraction (Figure 9) confirm the presence of more portlandite and ettringite in slurries with P1 ash than in slurries with P2 and P0 ash. Hardening slurries with the addition of ash with a coarser fraction of 30–100 µm are characterized by a rather loose microstructure, with larger gaps between the individual formations formed during the hydration of the binder. The morphology of the slurry microstructure with this ash (P2) corresponds to the relatively lower values of strength and hydraulic conductivity of these slurries. Figure 10 shows the microstructure of the hardening slurries with the addition of ash of the finer fraction 0–30 µm (Figure 10a) and the fraction 30–100 µm (Figure 10b). Photo "a" shows a tight C-S-H matrix with ettringite formations. Photo "b" shows the image of the C-S-H matrix and the spaces filled with ettringite crystals in the form of needles.

Slurry porosity tests performed by mercury porosimetry showed that the distribution of pores in the slurry and the size of the threshold diameter (Table 5) depend to a large extent on the size of ash grains. The threshold diameter is the size of the pores at which a step change in the volume of the injected mercury occurs, and it is also a measure of the continuity of the capillary pore system. The smaller the threshold diameter, the less continuous and finer the capillary porosity network. The highest value of the threshold diameter has slurries made with ash of the coarser fraction of 30–100 µm (P2). In the case of slurries based on P1 ash, the microstructure consists of finer elements, and thus the spaces between them are also smaller. In the case of slurries with the addition of P2 ash, we are dealing with thicker elements that build the microstructure, which translates into larger spaces between them. The values of the threshold diameter decreased with the increase in the dosing of the binder—Table 5.

Analyzing the hydraulic conductivity in correlation with the average values of the threshold diameters z and the share of the binder—Figure 11—it can be concluded that the formation of a more compact microstructure (more binder and smaller threshold diameter) is reflected in the reduced values of the hydraulic conductivity of the hardening slurries.

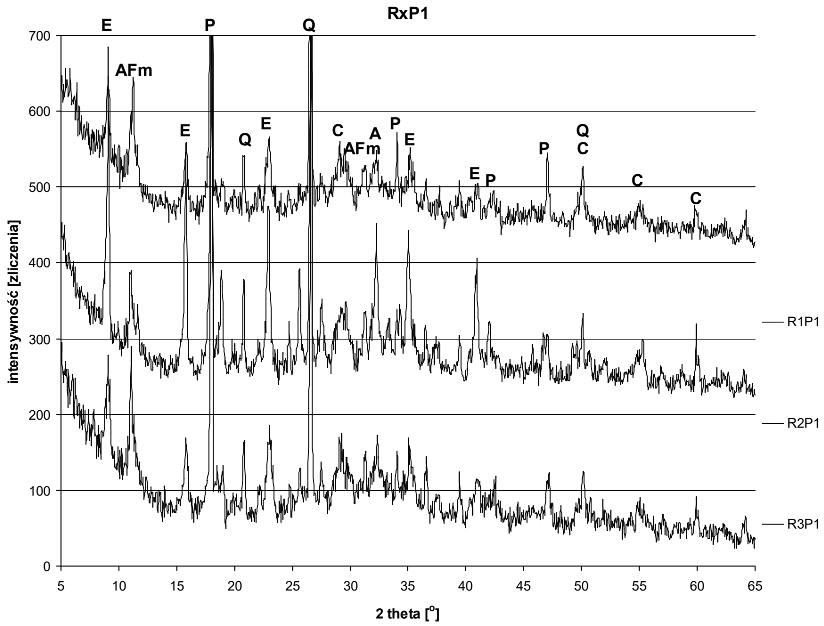

Figure 9. Diffractograms of samples of slurries with ashes of fraction 0–30 µm; E—ettringite, P—portlandite, AFm—hexagonal hydrated calcium aluminates, C–C-S-H phase, Q—quartz, A—alite.

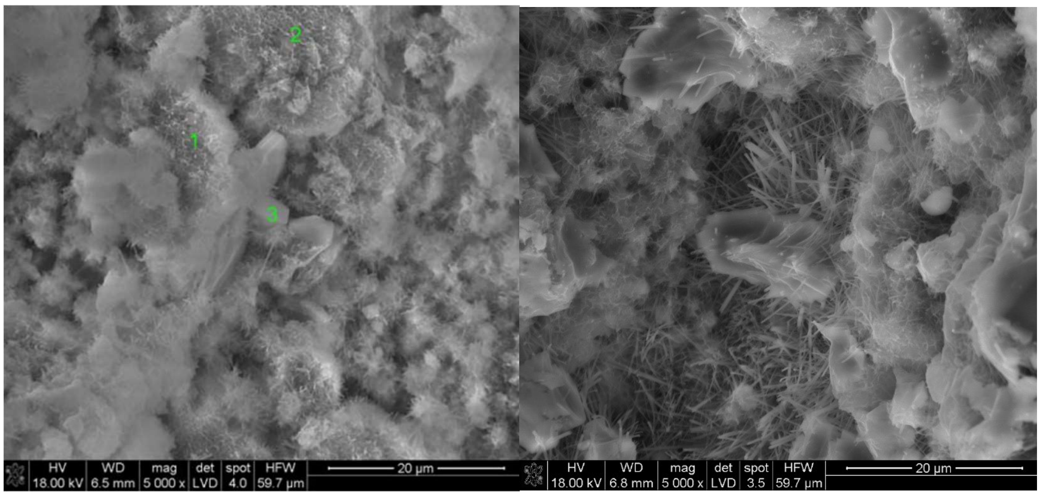

(**a**) (**b**)

Figure 10. Slurry microstructure: (**a**) R3P1, (**b**) R3P2 after 90 days of maturation.

Table 5. Threshold diameter values of hardening slurries.

Recipe	Sample Numbers	Threshold Diameter Values after 28 Days of Maturation [nm]	Threshold Diameter Values after 90 Days of Maturation [nm]
R1P1	1	4700	2500
R1P2	2	50,000	37,500
R1P0	3	12,500	6300
R2P1	4	3100	2000
R2P2	5	15,000	15,000
R2P0	6	10,600	5400
R3P1	7	2200	1200
R3P2	8	7500	7500
R3P0	9	6800	3800

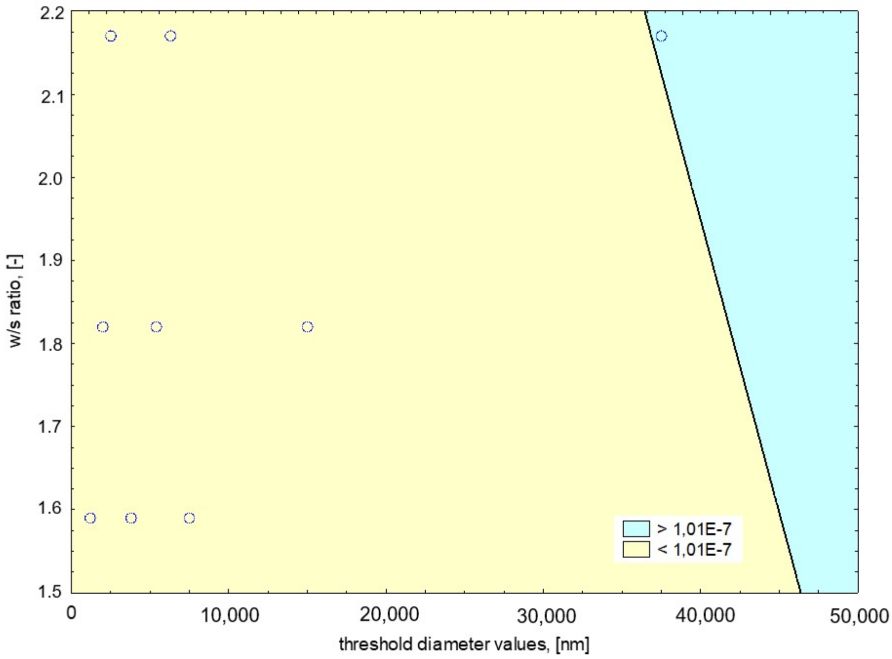

Figure 11. Relationship of hydraulic conductivity to threshold diameter values and w/s ratio.

4. Conclusions

The analysis of the properties of hardening slurries made with unfractionated and fractionated lignite ash in the grain size range of 0–30 µm and 30–100 µm and with Portland cement CEM I 42.5 and bentonite shows that almost all designed slurry compositions can be used in practice for sealing flood embankments, using various technologies for the implementation of cut-off walls in a soil medium. The criteria for designing the composition of the slurry are numerous due to the need to meet many requirements regarding the technological parameters of the liquid slurry as well as the mechanical and anti-filtration parameters of the hardened material in the cut-off wall. Taking into account the previously discussed criteria, it can be concluded that hardening slurries made with unfractionated ash (P0) and with ash with grains of a coarser fraction of 30–100 µm (P2) do not present hydraulic conductivity at the usually required level of 10^{-8} m/s, which limits the possibilities of their use in cut-off walls. The hardening slurries made with the ash of the finer fraction of 0–30 µm (P1) were the most favorable, which results from the higher content of colloidal particles and the pozzolanic activity of this material. In the case of slurries from the P1 group, each method of making a cut-off wall can bring the expected results, i.e., ensure the obtained barriers with sufficiently low hydraulic conductivity and sufficiently high mechanical strength at a level that ensures proper cooperation of the barrier with the soil.

Author Contributions: Conceptualization, P.F. and A.M.; methodology, P.F. and A.M.; software, P.F.; validation, P.F. and A.M.; formal analysis, Z.K. and P.F.; investigation, P.F. and A.M.; resources, A.M.; data curation, A.M.; writing—original draft preparation, P.F. and AM.; writing—review and editing, Z.K.; visualization, P.F.; supervision, Z.K.; project administration, P.F.; funding acquisition, P.F. All authors have read and agreed to the published version of the manuscript.

Funding: Investigations were carried out as part of the IniTech programme No. ZPB/61/65832/IT2/10.

Data Availability Statement: The data presented in this study are available on request from the corresponding author.

Conflicts of Interest: The authors declare no conflict of interest.

References

1. *PN-EN 14679:2005*; Execution of Special Geotechnical Work—Deep Soil Mixing. European Standards: Plzen, Czech Republic, 2005.
2. Topolnicki, M. Geotechnical Design and Performance of Road and Railway Viaducts Supported on DSM Columns—A Summary of Practice. In Proceedings of the International Conference on Deep Mixing, San Francisco, CA, USA, 2–5 June 2015.
3. Kledyński, Z.; Rafalski, L. Hardening slurries. In *KILiW PAN, IPPT. 254*; Polish Academy of Sciences, Comitee of Civil Engineering: Warsaw, Poland, 2009. (In Polish)
4. Kledyński, Z.; Falaciński, P.; Machowska, A.; Dyczek, J.; Kotwica, Ł. Utilisation of CFBC fly ash in hardening slurries for flood-protection dikes. *Arch. Civ. Eng.* **2016**, *LXII*, 75–87. [CrossRef]
5. *PN-EN 12716:2019-01*; Execution of Special Geotechnical Work—Jet Grouting. European Standards: Plzen, Czech Republic, 2019.
6. Ochmański, M.; Modini, G.; Bzówka, J. Prediction of the diameter of jet grouting columns with artifical neural networks. *Soils Found.* **2015**, *55*, 425–436. [CrossRef]
7. Evans, J.; Dawson, A.; Opdyke, S. Slurry walls for groundwater control: A comparison of UK and US practice. In Proceedings of the ASCE/PENNDOT Central PA Geotechnical Conference, Hershey, PA, USA, 29–31 October 2002.
8. Rafalski, L. Properties and applications of hardening slurries. In *Archives of Hydro-Engineering and Environmental Mechanics*; Instytut Badawczy Dróg i Mostów: Warszawa, Poland, 1995. (In Polish)
9. Falaciński, P. Leak tightness of hardening slurries with fluidal fly ashes in chemically aggressive environments. *Arch. Environ. Prot.* **2011**, *37*, 115–134.
10. Kledyński, Z.; Falaciński, P.; Machowska, A.; Szarek, Ł.; Krysiak, Ł. Hardening slurries with fluidized-bed combustion by-products and their potential significance in terms of circular economy. *Material* **2021**, *14*, 2104. [CrossRef] [PubMed]
11. Giergiczny, Z. Fly ash and slag. *Cem. Concr. Res.* **2019**, *124*, 105826. [CrossRef]
12. Giergiczny, Z.; Król, A.; Tałaj, M.; Wandoch, K. Performance of concrete with low CO_2 emission. *Energies* **2020**, *13*, 4328. [CrossRef]
13. *BN-90/1785-01:1990*; Drilling Rinse. Field Test Methods. (In Polish)
14. *PN-85/G-02320:1985*; Drilling. Cements and Grouts for Cementing in Boreholes. Polish Committee for Standardization: Warsaw, Poland, 1985. (In Polish)
15. *PN-EN 12390-3:2019*; Testing Hardened Concrete—Part 3: Compressive Strength of Test Specimens. European Standards: Plzen, Czech Republic, 2019.
16. *PN-EN 12390-6:2011*; Testing Hardened Concrete—Part 6: Tensile Splitting Strength of Test Specimens. European Standards: Plzen, Czech Republic, 2011.
17. Falaciński, P.; Kledyński, Z. Impact of acid aggressiveness on the filtration resistance of hardening slurries with an addition of fluidized-bed fly-ash. *Arch. Civ. Eng.* **2021**, *67*, 475–490. [CrossRef]
18. Zhang, Z.; Dai, Z.; Sheng, Y. Study on the Permeability of Modified Bentonite Slurry in Landfill. *Adv. Mater. Sci. Eng.* **2020**, 8970270. [CrossRef]
19. Zabielska-Adamska, K. Hydraulic conductivity of fly ash as a barrier material: Some problems in determination. *Environ. Earth Sci.* **2020**, *79*, 321. [CrossRef]